

The MUSE Detector System

Roland Reiss (rreiss@eso.org), Sebastian Deiries, Jean-Louis Lizon, Gero Rupprecht
European Organisation for Astronomical Research in the Southern Hemisphere
Karl-Schwarzschild-Strasse 2, D-85748 Garching bei München

Abstract *MUSE (Multi Unit Spectroscopic Explorer) is a second generation instrument for the VLT. It is built by a consortium of European institutes and ESO. MUSE consists of 24 Integral Field Units each equipped with its own cryogenically cooled CCD head. The detectors used are deep depletion e2v CCD231-84 with 15 μm pixels and 4096x4112 active pixels. After passing Final Design Review in early 2009 the MUSE Instrument Detector System (IDS) is now in the production phase.*

The paper gives an overview of the complex MUSE IDS including detector controllers, the cryogenic and vacuum system and the precision assembly of CCDs into the 24 detector heads.

We present results from the characterization of the first science grade e2v CCDs. These CCDs have a graded anti-reflection coating which is matched to the MUSE spectrographs.

1 Instrument

MUSE is an integral field spectrometer to be mounted on the Nasmyth platform of one of the VLT UTs. The Fore Optics splits a large field of view into 24 sub-fields. 24 Integral Field Units provide the spectral decomposition of the sub fields. Each IFU includes its own Instrument Detector Subsystem (IDS). The spectral coverage is 465 to 930 nm.

2 Instrument Detector System (IDS)

The Detector Controller (ESO's New General detector Controller NGC) consists of a total number of 24 Front-end Basic Boards (FEBs) in four 6-slot housings. Each FEB contains sequencer, bias and clock circuitry, and a 4-channel video chain with clamp/sample circuit and 16-bit ADCs. Figure 1 shows an overview of a 6-slot NGC.

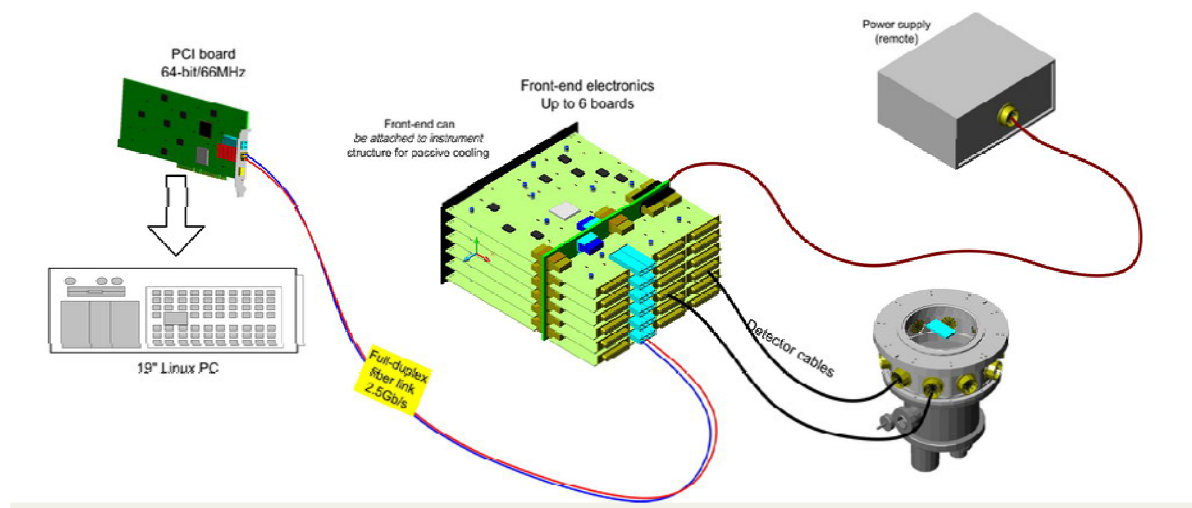


Figure 1 Instrument Detector System (Overview)

3 Detectors

The detectors for MUSE are manufactured by *e2v technologies*. The design is based on the 4Kx4K deep depletion backside illuminated CCD231-84. As the MUSE spectrographs have a fixed spectral format the CCDs have been coated with a graded anti-reflection coating (Figure 2).

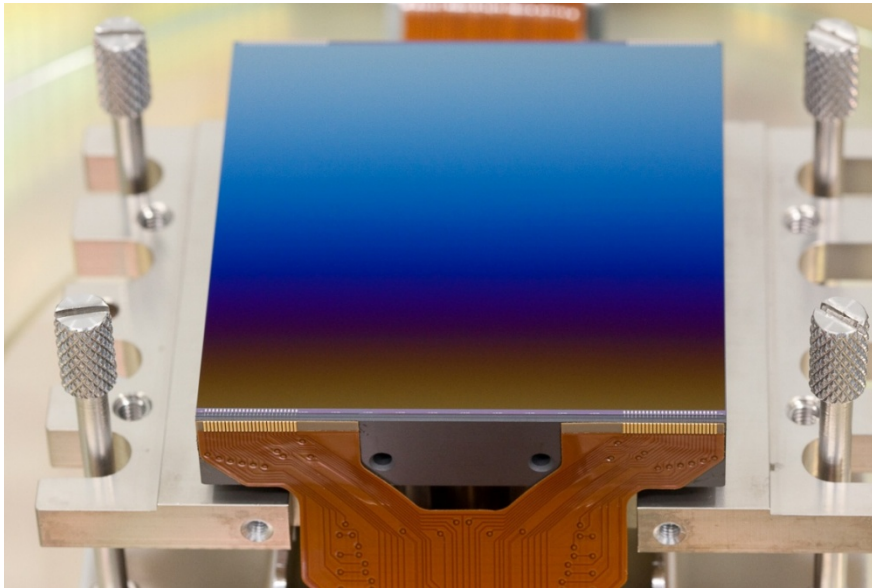


Figure 2 CCD231-84 with graded AR coating

The package (Figure 3) is made from silicon carbide (SiC) and has excellent thermal and mechanical properties. The surface flatness is within $\pm 10\mu\text{m}$.

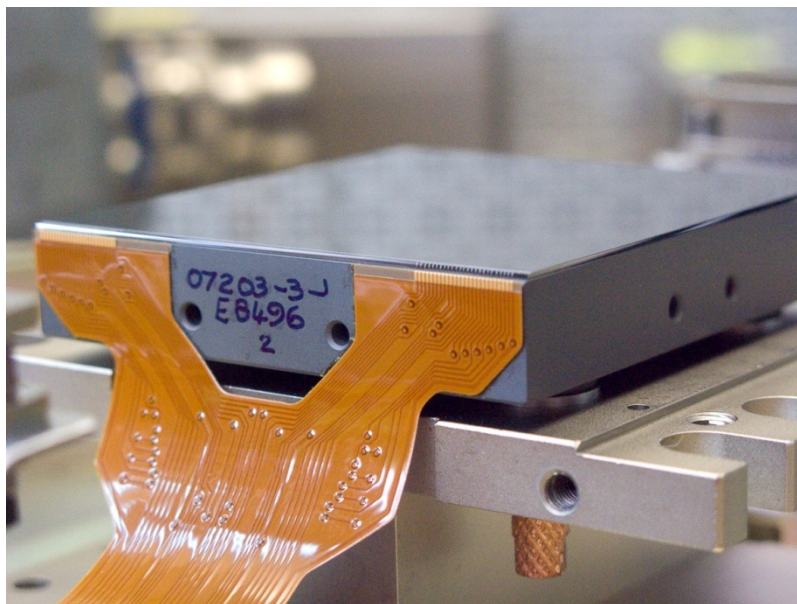


Figure 3 SiC package with flexboard interconnects

Figure 4 shows a detector head after assembly.



Figure 4 Assembled detector head

4 Summary of detector properties

Table 1 lists the key properties of the MUSE detectors. The values are based on measurements from three out of 24 science grade devices.

Item	Value
Type	e2v CCD231-84, deep depletion, backside illuminated, graded AR coating
Format	4096x4112, 4 outputs + 4 dummy outputs
Pixel size	15 x 15 μm^2
Noise	< 3e ⁻ RMS @ 100kpix/sec (default readout mode for science exposures) < 4e ⁻ RMS @ 200kpix/sec < 5e ⁻ RMS @ 500kpix/sec
Readout time	< 10sec @ 500kpix/sec (4 ports)
Linearity error	< $\pm 0.4\%$ @ 100kpix/sec
Quantum efficiency	> 90% (460..780nm) > 60% @ 900nm > 40% @ 930nm
AR coating	Graded coating, matched to MUSE spectral coverage (465..930nm)
Dark current	< 3 e ⁻ /pix/hour @ 163K
CTE	> 0.999995 (v/h) (e2v data)
Point Spread Function	See Figure 11 to Figure 13
Package	SiC, 4-side buttable, two flex boards with 37-pin Micro D connectors
Flatness	< 20 μm peak-to-valley, including package tolerances.
Operating temperature	163K

Table 1 Summary of detector properties

5 Detector Results

5.1 Quantum Efficiency

Figure 5 shows the quantum efficiency (QE) of CCD „Psyche“. The red (ESO) and green (e2v) curves show the QE at the „optimum“ position of the graded AR coating. The blue curve is the QE averaged over the whole device.

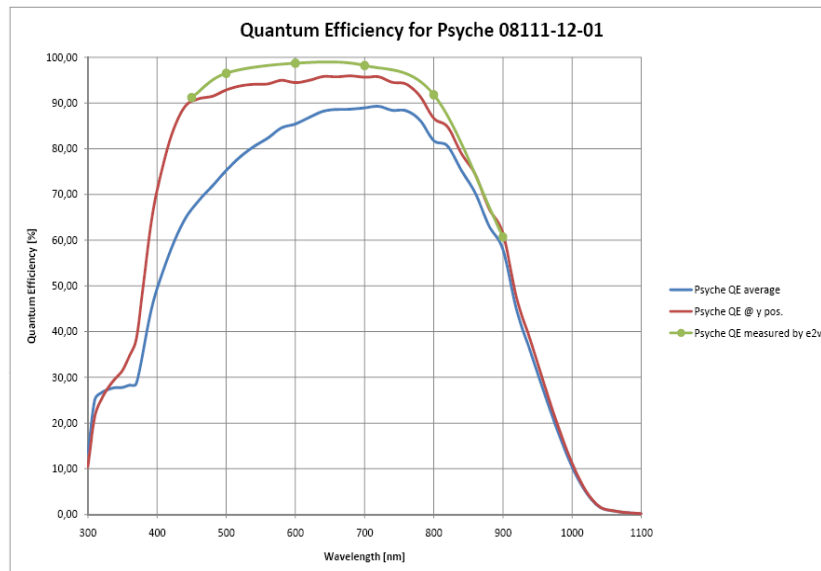


Figure 5 Quantum efficiency of CCD "Psyche"

Figure 6 shows a plot of the „optimum position“ QE of three different devices („Juno“, „Psyche“ and „Urania“). The close match of QE values is quite remarkable.

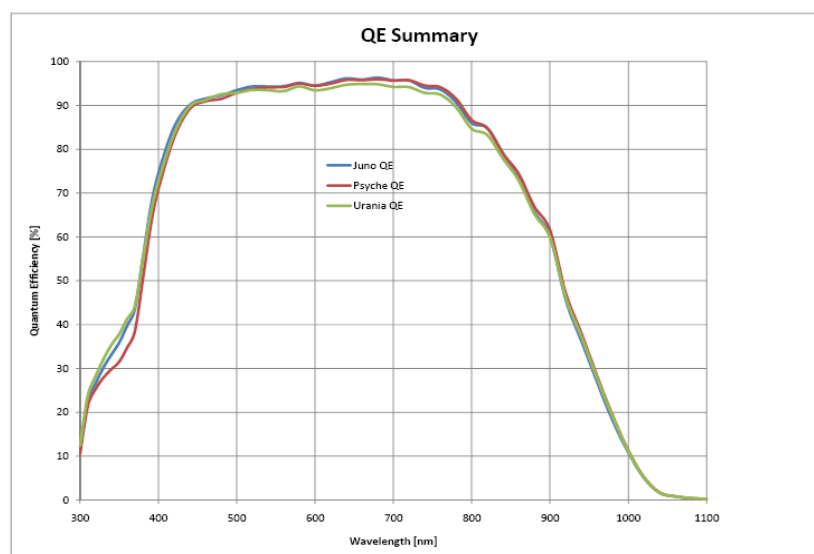


Figure 6 QE comparison of CCDs "Psyche", "Juno" and "Urania"

The 2-D plots in Figure 7 illustrate the effect of the graded AR coating over the whole imaging area at 400, 500, 600 and 800nm.

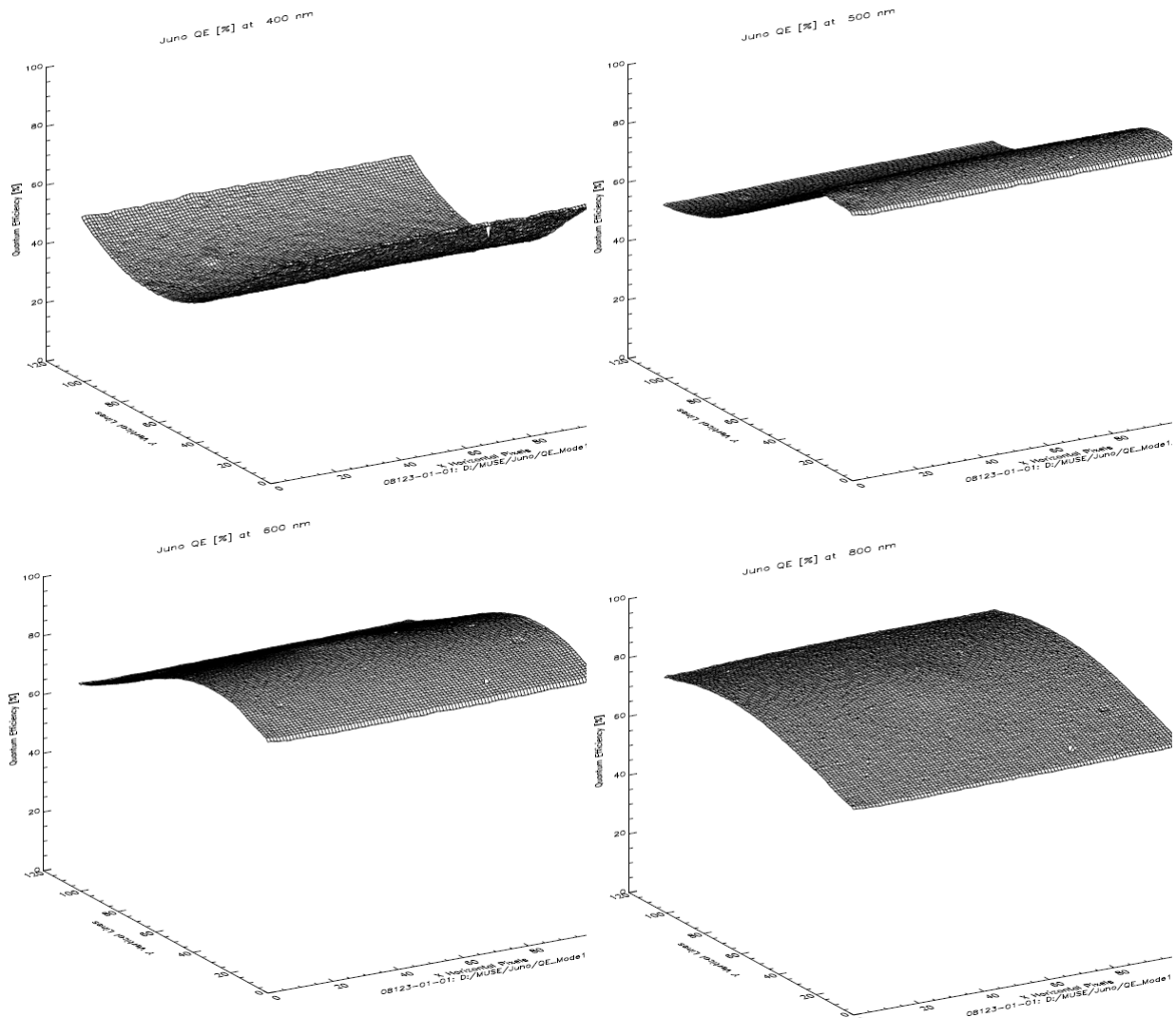


Figure 7 2-D QE plots for 400, 500, 600 and 800nm

5.2 Linearity

Figure 8 shows the linearity error of the four output ports of CCD „Psyche“ within a range of approx. 140 to 40,000 e^- at a binning of 4x4 and 100kpix/sec readout speed. 4x4 binning improves the linear relationship of signal variance vs. mean signal and gives a calibration of the conversion factor. See [1] for details.

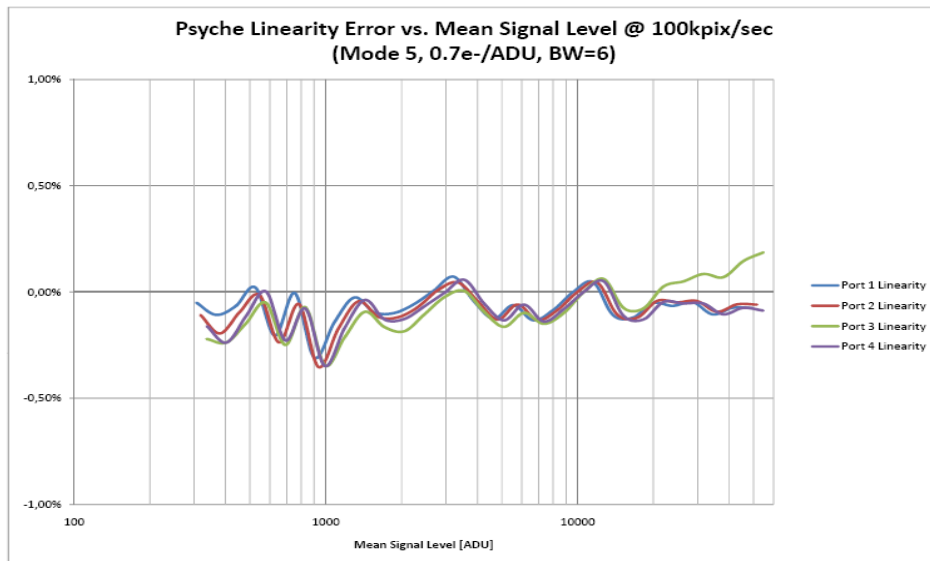


Figure 8 Linearity error of "Psyche"

5.3 Point Spread Function

The technique used is loosely based on the Foucault knife-edge technique. A spot projected onto the CCD (Figure 9) is stepped across the CCD in small increments ($1\mu\text{m}$) in the row (Y) or column (X) direction using an XYZ stage (Figure 10). As the spot is scanned into a small subregion of pixels, the edge of which acts like a virtual knife edge, the charge in this small subregion is measured. More details can be found in [2].

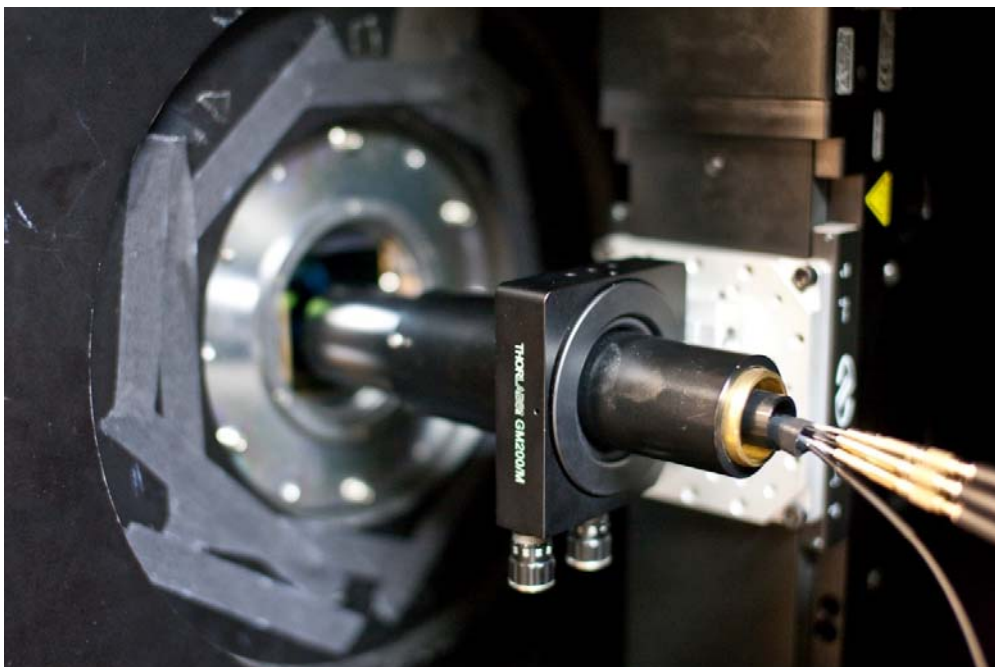


Figure 9 Spot projector for PSF measurements

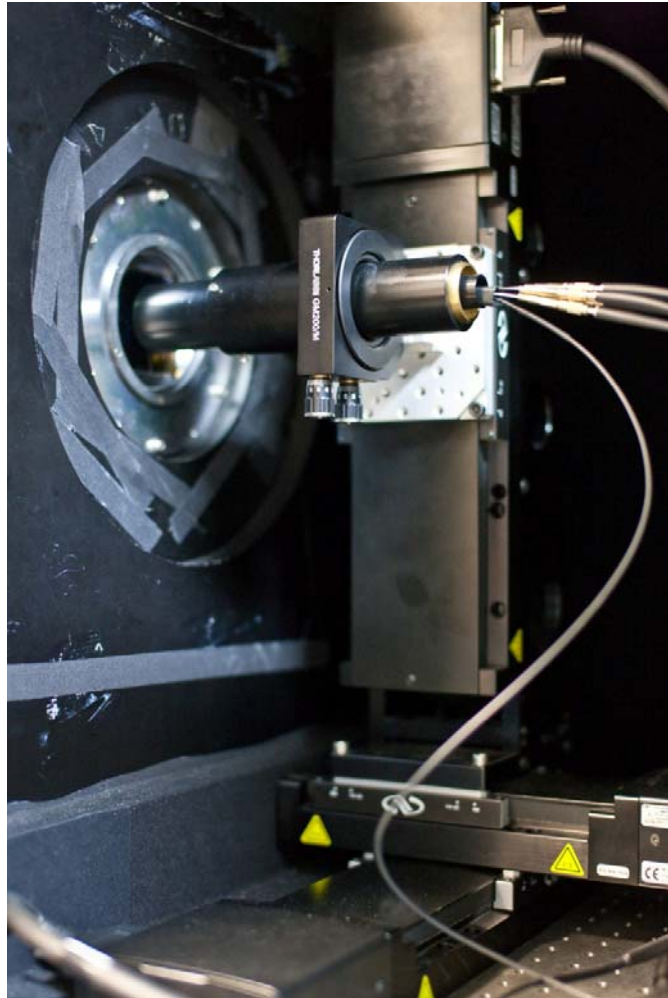


Figure 10 XYZ stage

The PSF values have been measured with several CCD231-84 devices at different values of the collection phase voltage V_c . This is the “high” value of the vertical clocks. The “low” value of the vertical clocks remains unchanged at -8V. $V_c = 2V$ is the nominal operating voltage.

Data reduction was done with kind support from Mark Downing, ESO. The results are presented in Figure 11, Figure 12 and Figure 13. The PSF values measured for “Psyche” are significantly worse than the ones of “Ceres” and “Juno”. Measurements of a fourth device (“Fortuna”, not shown here) however confirm the better results of “Ceres” and “Juno”.

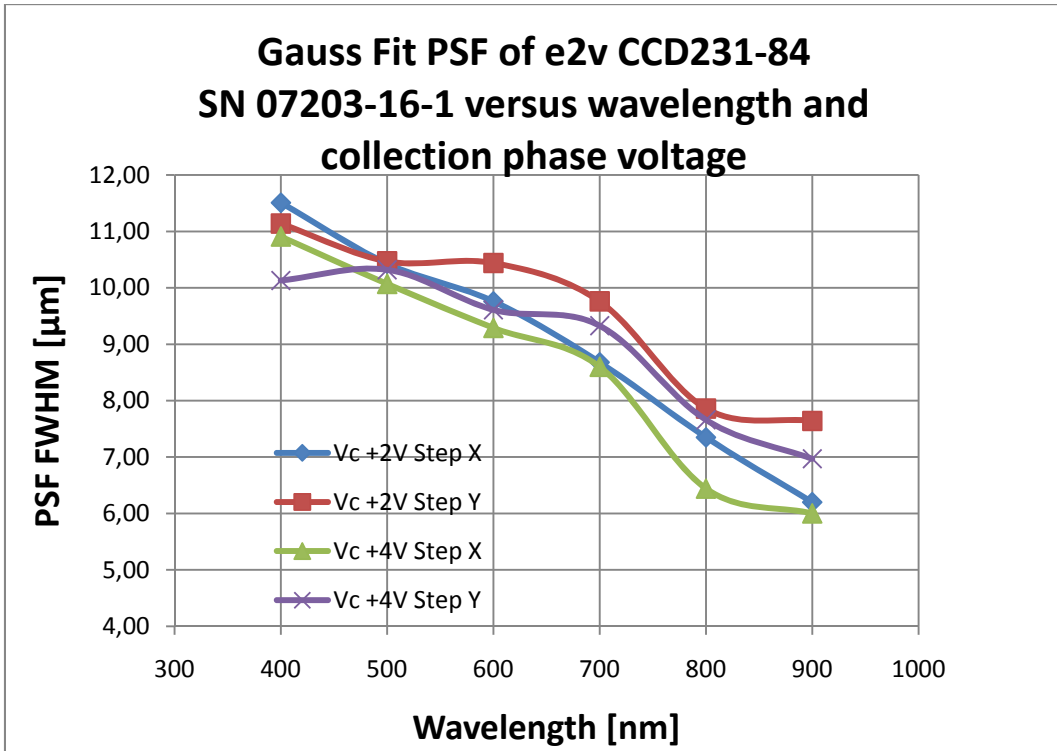


Figure 11 Point Spread Function of "Ceres"

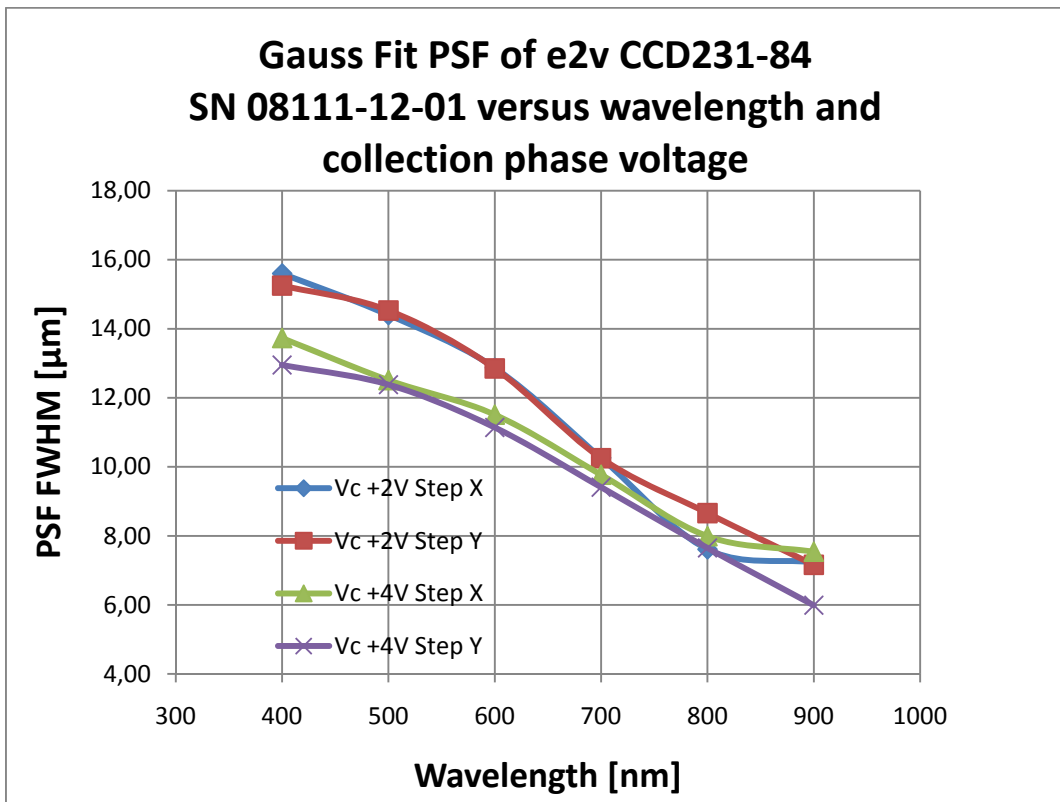


Figure 12 Point Spread Function of "Psyche"

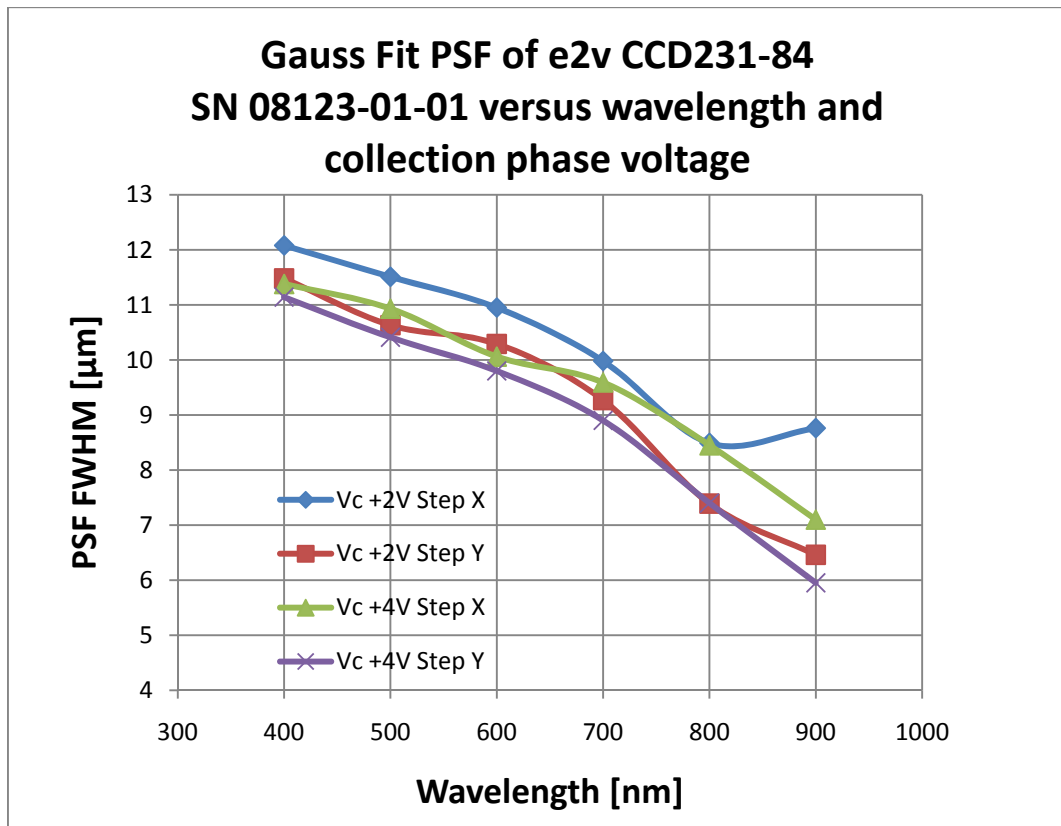


Figure 13 Point Spread Function of "Juno"

6 Vacuum and Cryogenic System (VCS)

Each of the 24 detectors is mounted in its own Detector Vessel (DV) shown in Figure 14. The Detector Vessel consists of the Detector Head and a liquid nitrogen (LN2) cooled Continuous Flow Cryostat (CFC).



Figure 14 Detector Vessel (head and CFC)

The thermal control of the 24 detector heads and cryostats is handled by a unit named „TeePee“. TeePee is based on an industrial Program Controller (JUMO Imago 500). One TeePee contains two Imago 500 and controls and monitors two detector vessels.

TeePee (Figure 15) is made from industrial components (controller, power supplies, solid state relays).



Figure 15 TeePee

The Imago 500 (Figure 16) controls and monitors

- Detector temperature
- Cold plate temperature
- N2 exhaust gas temperature
- Sorption pump temperature during regeneration
- Vacuum pressure (Edwards WRG)

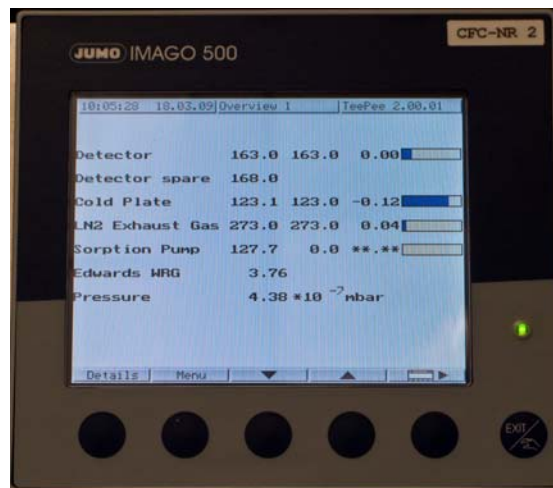


Figure 16 Imago 500 front panel

There are numerous interlocks for temperature and pressure to guarantee detector safety. All TeePees are connected via Profibus-TP to a master controller (Siemens PLC).

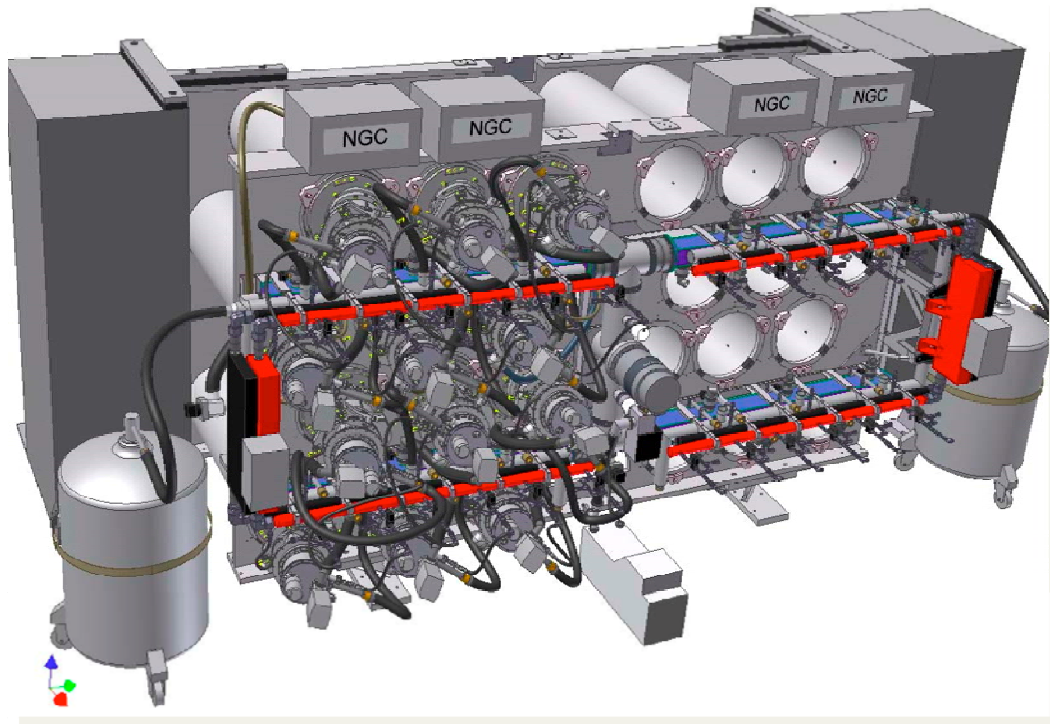


Figure 17 Instrument Main Structure

The drawing in Figure 17 shows the Instrument Main Structure (IMS) with 12 out of 24 Detector Vessels installed. The four 6-slot NGCs are on top, the blue parts are the vacuum lines. The red pipes collect the N2 exhaust gas which is used to flush the instrument. The grey lines are for LN2 distribution. The control electronics (TeePees) are located in the cabinets to the left and right.

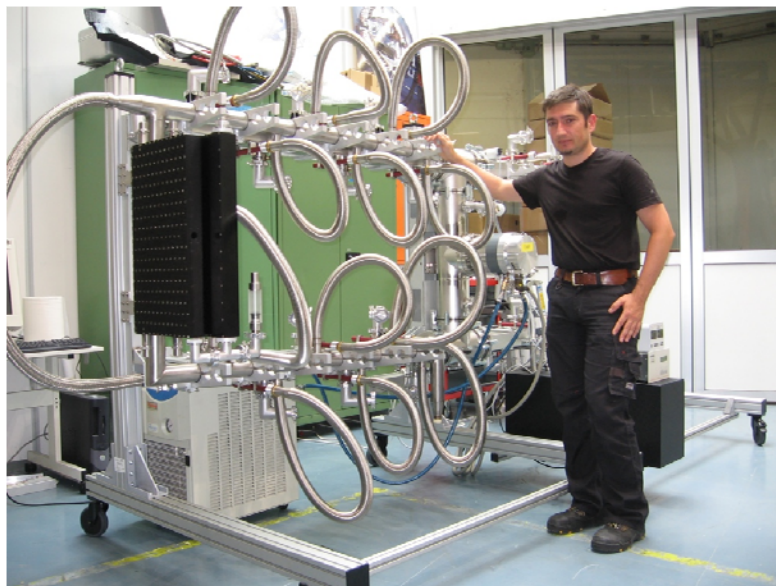


Figure 18 Vacuum and Cryogenic System

Figure 18 shows the LN2 and vacuum distribution lines currently being integrated in the ESO Assembly Hall. Initial tests for the VCS are foreseen for late 2009.

The 24 detectors and related infrastructure will be delivered to CRAL between Q1 2010 and Q3 2011 at an approximate pace of 2 units per month.

7 References

1. Downing, Mark; Baade, Dietrich; Sinclair, Peter; Deiries, Sebastian; Christen, Fabrice. High Energy, Optical, and Infrared Detectors for Astronomy II. Edited by Dorn, David A.; Holland, Andrew D.. Proceedings of the SPIE, Volume 6276, pp. 627609 (2006).
2. M.D. Downing; Investigation of PSF of CCDs; VLT-TRE-ESO-13600-4317,